

Synthesis of Low-Polydispersity Poly(*N*-ethylmethacrylamide) by Controlled Radical Polymerizations and Their Thermal Phase Transition Behavior

JIAN XU, XIAOZE JIANG, SHIYONG LIU

Department of Polymer Science and Engineering, Hefei National Laboratory for Physical Sciences at the Microscale, University of Science and Technology of China, Hefei, Anhui 230026, China

Received 23 July 2007; accepted 17 August 2007

DOI: 10.1002/pola.22358

Published online in Wiley InterScience (www.interscience.wiley.com).

ABSTRACT: Controlled radical polymerizations of *N*-ethylmethacrylamide (EMA) by atom transfer radical polymerization and reversible addition-fragmentation chain transfer processes were investigated in detail for the first time, employing complementary characterization techniques including gel permeation chromatography, ¹H NMR spectroscopy, and matrix-assisted laser desorption ionization time-of-flight mass spectrometry. In both cases, relatively good control of the polymerization of EMA was achieved, as revealed by the linear evolution of molecular weights with monomer conversions and the low polydispersity of poly(*N*-ethylmethacrylamide) (PEMA). The thermal phase transitions of well-defined PEMA homopolymers with polydispersities less than 1.2 and degrees of polymerization up to 320 in aqueous solution were determined by temperature-dependent turbidity measurements. The obtained cloud points (CPs) vary in the range of 58–68 °C, exhibiting inverse molecular weight and polymer concentration dependences. Moreover, the presence of a carboxyl group instead of an alkyl one at the PEMA chain end can elevate its CP by ~3–4 °C. © 2007 Wiley Periodicals, Inc. *J Polym Sci Part A: Polym Chem* 46: 60–69, 2008

Keywords: living radical polymerization (LRP); phase behavior; stimuli-sensitive polymers

INTRODUCTION

Thermoresponsive water-soluble polymers have attracted ever-increasing attention within the past decade because of their diverse applications in fields of biomedicines, biosensing, soft actuators/valves, and catalysis.¹ Most of them exhibit an inverse temperature dependence on the solubility in aqueous solutions, that is, a lower critical solution temperature (LCST). Below the LCST,

these polymers are soluble because of hydrogen bonding interactions between hydrophilic groups and water. At elevated temperatures (above the LCST), hydrogen bonds are weakened and hydrophobic interactions between adjacent groups dominate, leading to the collapse and aggregation of polymer chains and eventual macroscopic phase separations.

Among those previously studied systems, thermal phase transitions of water-soluble polymers based on acrylamido monomers have been extensively investigated. They can be further categorized into two main types: *N*-monosubstituted acrylamide and *N,N*-disubstituted acrylamide polymers. The LCSTs of poly(*N*-monosubstituted

Correspondence to: S. Liu (E-mail: sliu@ustc.edu.cn)

Journal of Polymer Science: Part A: Polymer Chemistry, Vol. 46, 60–69 (2008)
© 2007 Wiley Periodicals, Inc.

acrylamide) polymers mainly depend on the monomer structures. Polyacrylamide and poly(*N*-methylacrylamide) are water-soluble and do not exhibit LCST phase behavior, whereas poly(*N*-*n*-butylacrylamide) and poly(*N*-*t*-butylacrylamide) are water-insoluble. Interestingly, poly(*N*-ethylacrylamide), poly(*N*-isopropylacrylamide) (PNIPAM), and poly(*N*-*n*-propylacrylamide) exhibit decreasing LCSTs, being ~74, 32, and 22 °C, respectively. This apparently indicates that the LCSTs decrease with increasing hydrophobicity of the substituted alkyl groups in repeating units.²

On the other hand, the thermal phase transitions of these polymers also depend on the molecular weight (MW), concentration, terminal groups, and the presence of small molecule additives.^{3–8} Recently, Stover and coworkers^{9,10} successfully synthesized a series of low-polydispersity PNIPAM with different MWs and varying end groups by atom transfer radical polymerization (ATRP). They found that the thermal phase transition temperatures, that is, cloud points (CPs), of PNIPAM homopolymers can vary in the broad temperature range of 32–70 °C, depending on their MWs and hydrophobicity of end groups.

Compared with that of poly(*N*-monosubstituted acrylamide) such as PNIPAM,^{11–14} the thermal phase transition behavior of poly(*N,N*-disubstituted acrylamides) has been less explored. As the latter does not contain amide protons, hydrogen bonding interactions between chain segments are much weaker than that of the former, leading to unique thermal phase transitions. For example, poly(*N,N*-dimethylacrylamide) (PDMA) is water-soluble up to 100 °C, whereas the CPs of poly(*N,N*-diethylacrylamide) (PDEA) in aqueous solution were reported to range from 25 to 40 °C, depending on the heating rate, polymerization method, and the presence of additives.^{3,15–17} It should be noted that almost all the reported PDEA homopolymers were prepared by conventional free radical polymerization, leading to polymers with quite broad molecular weight distributions. Thus, it is difficult to extract the effect of a single parameter on their thermal phase transitions.

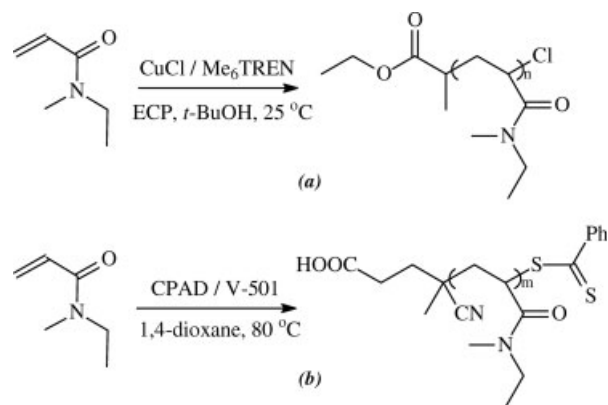
We are interested in the thermal phase transition of poly(*N*-ethylmethacrylamide) (PEMA) homopolymers. Based on chemical intuition, the CP values should lie between those of PDMA and PDEA. Preliminary literature surveys revealed that the aqueous solution properties of PEMA have not been systematically studied. Ito et al.¹⁸ reported a CP value of 56 °C for PEMA

prepared by conventional free radical polymerization, whereas Freitag and coworkers¹⁹ reported a CP value of 75 °C for fractionated PEMA samples with relatively low MW. This indicates that a more detailed investigation is highly desirable to elucidate the effects of MWs and end groups of PEMA on their thermal phase transitions.

Thus, low-polydispersity PEMA samples with varying MWs are needed for this study. Nakahama and coworkers²⁰ reported that the anionic polymerization of EMA initiated by diphenylmethylpotassium in THF. They also found that diethylzinc can enhance the control of polymerization, resulting in PEMA homopolymers with low polydispersities and predetermined MWs. However, this technique requires quite stringent reaction conditions to avoid side reactions such as chain termination and/or chain transfer.

Recent advances in controlled radical polymerizations (CRP) such as nitroxide-mediated radical polymerization (NMRP), ATRP, and reversible addition-fragmentation chain transfer (RAFT) polymerization seem to be able to provide a suitable approach to solve this problem. Successful ATRP and RAFT polymerizations of *N,N*-dimethylacrylamide (DMA) and *N,N*-diethylacrylamide (DEA) with good control over the MWs and polydispersities have been previously reported by research groups of Matyjaszewski and coworkers,^{21–24} Brittain and coworkers,^{25,26} McCormick and coworkers,^{27–30} and Thang and coworkers^{31,32} As EMA is structurally similar to that of DMA and DEA monomers, the controlled radical polymerization of DMA via ATRP and RAFT processes should be feasible. Just recently, Zhu and coworkers³³ synthesized triblock copolymers containing PEMA blocks by consecutive RAFT polymerizations; however, detailed polymerization kinetics of EMA was not provided.

Herein, we present a full investigation of the feasibility of controlled radical polymerizations of EMA monomer via ATRP and RAFT processes (Scheme 1), and the polymerization kinetics was studied in detail. Moreover, the thermal phase transitions of low-polydispersity PEMA homopolymers were investigated by temperature-dependent turbidimetry. The effects of MWs, polymer concentrations, and end groups on the CPs of PEMA were elucidated. We found that a combination of these parameters results in sharp thermal phase transitions, and the LCSTs can be tuned in the temperature range of 58–68 °C.



Scheme 1. Schematic illustration of the syntheses of well-defined poly(*N*-ethylmethacrylamide) (PEMA) homopolymers via (a) ATRP and (b) RAFT processes.

EXPERIMENTAL

Materials

N-Ethylmethacrylamide (97%), acryloyl chloride (96%), copper(I) chloride (CuCl, 99.99%), and ethyl 2-chloropropionate (ECP) (97%) were all purchased from Aldrich and were used as received. Tris(2-aminoethyl)amine (TREN, 96%) was purchased from Acros and used as received. 4,4'-Azobis(4-cyanopentanoic acid) (V-501, Acros) was recrystallized from methanol before use. Tris(2-(dimethylamino)ethyl)amine (Me₆TREN) and 4-cyanopentanoic acid dithiobenzoate (CPAD) were prepared according to literature procedures.^{34,35} All other reagents were purchased from Sinopharm Chemical Reagent and used as received.

Sample Synthesis

Synthesis of *N*-Ethylmethacrylamide

EMA was prepared by the reaction of *N*-ethylmethacrylamide with acryloyl chloride. Typically, *N*-ethylmethacrylamide (11.82 g, 0.2 mol) and triethylamine (20.24 g, 0.2 mol) were mixed with 500 mL dry ethyl ether. After cooling to 0 °C, acryloyl chloride (18.10 g, 0.2 mol) was added dropwise over 60 min. Magnetic stirring was continued for 12 h at room temperature. After removing the precipitated ammonium salt by suction filtration and evaporating out solvents, the crude product was further purified by silica gel column chromatography using dichloromethane as the eluent. After removing dichloromethane by rotary evaporator, the remaining residues were distilled under reduced pressure

in the presence of a small amount of hydroquinone. A colorless liquid was obtained with an overall yield of ~75%. ¹H NMR (CDCl₃, δ, ppm): 1.1–1.2 (m, 3H, CH₃), 2.9–3.1 (s, 3H, NCH₃), 3.3–3.5 (m, 2H, NCH₂), 5.6–5.7 (dd, 1H, *cis* β-CH₂), 6.2–6.3 (dd, 1H, *trans* β-CH₂), 6.5–6.6 (dd, 1H, α-CH) [Fig. 1(a)].

General Procedures for ATRP of EMA

To achieve a target degree of polymerization (DP) of 80, the mixture containing EMA (3.63 g, 32 mmol), Me₆TREN (92 mg, 0.4 mmol), and *tert*-butyl alcohol (7.26 g) was deoxygenated by bubbling with nitrogen for at least 20 min. CuCl (40 mg, 0.4 mmol) was then introduced under the protection of N₂ flow. The reaction mixture was stirred for ~10 min to allow the formation of CuCl/Me₆TREN complex. Ethyl 2-chloropropionate (54 mg, 0.4 mmol) was then injected via a syringe to start the polymerization. The polymerization was conducted at 25 °C under magnetic stirring. Aliquots (0.5 mL) were withdrawn from the reaction mixture at predetermined time intervals and divided into two portions. One portion was directly diluted with D₂O for ¹H NMR analysis to determine monomer conversions. The other portion was diluted with THF and passed through a short neutral alumina column to remove copper catalysts. After removing the solvents, the residues were subjected to GPC analysis.

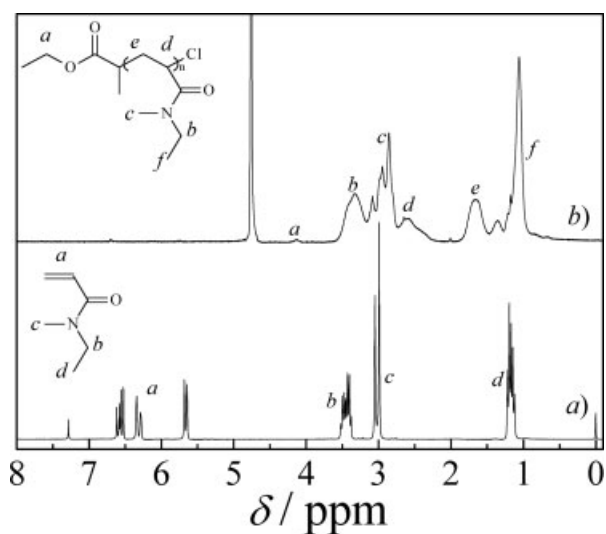


Figure 1. ¹H NMR spectra of (a) EMA monomer in CDCl₃ and (b) PEMA homopolymer prepared via ATRP in D₂O.

After polymerization at 25 °C for 6 h, the final product was obtained by passing through neutral alumina column and precipitating into anhydrous ethyl ether for three times. The obtained PEMA was dried in a vacuum oven at room temperature for 12 h.

General Procedure for RAFT Polymerization of EMA

The RAFT polymerization of EMA monomer was conducted at 80 °C in 1,4-dioxane, employing V-501 as the source of primary radicals and CPAD as the chain transfer agent. A homogeneous mixture containing EMA (11.32 g, 0.1 mol), CPAD (70 mg, 0.25 mmol), V-501 (14 mg, 0.05 mmol), and 1,4-dioxane (22 mL) was evenly distributed into seven glass ampoules equipped with magnetic stir bars. The molar ratio of [EMA]:[CPAD]:[V-501] was 2000:5:1 in the reaction mixture. The ampoules were subjected to three freeze-thaw cycles, flame-sealed under vacuum, and then immersed into an oil bath thermostated at 80 °C to start the RAFT polymerization. At predetermined time intervals, glass ampoules were taken out and quenched into liquid nitrogen to terminate the polymerization. Monomer conversions were determined by ¹H NMR in CDCl₃ for the unpurified samples. The reaction mixture was then diluted with THF and precipitated into an excess of anhydrous ethyl ether for three times. The obtained PEMA was dried in a vacuum oven at room temperature for 12 h. MWs and polydispersities of the final products obtained at different monomer conversions were determined by DMF GPC.

Characterization

Nuclear Magnetic Resonance Spectroscopy

All ¹H NMR spectra were recorded in CDCl₃ or D₂O at 25 °C on a Bruker AV300 NMR spectrometer (resonance frequency of 300 MHz for ¹H) operating in the Fourier transform mode.

Gel Permeation Chromatography

MWs and molecular weight distributions were determined by GPC using a series of three linear Styragel columns (HT2, HT4, and HT5) and an oven temperature of 50 °C. Waters 1515 pump and Waters 2414 differential refractive index detector (set at 30 °C) were used. The elu-

ent was DMF at a flow rate of 1.0 mL/min. The calibration was based on seven polystyrene standards with the molar masses ranging from 1310 to 3,740,000 g/mol.

Matrix-Assisted Laser Desorption/Ionization Time-of-Flight Mass Spectrometry

The MALDI-TOF mass spectrum was recorded in the linear mode on a Bruker BIFLEXe III mass spectrometer using a nitrogen laser (337 nm) and an accelerating potential of 20 kV. 2,5-Dihydroxybenzoic acid (DHB) (99%, Sigma) was used as the matrix and NaBF₄ was added to improve the ionization.

Temperature-Dependent Turbidimetry

The optical transmittance of aqueous solutions of PEMA at a wavelength of 500 nm was acquired on a Unico UV/vis 2802PCS spectrophotometer. A thermostatically controlled cuvette was employed and the heating rate was 0.2 °C/min. CP value of the aqueous PEMA solution at a specific concentration was determined as the temperature corresponding to ~10% decrease of the optical transmittance.

RESULTS AND DISCUSSION

As shown in Scheme 1, two synthetic pathways, ATRP and RAFT, were attempted for the controlled radical polymerizations of EMA to prepare low-polydispersity PEMA samples with predetermined MWs. ECP and CPAD were employed as the initiator of ATRP and chain transfer agent of RAFT polymerization, respectively. Thus, the obtained polymers will differ in terminal end groups. The RAFT polymerization of EMA in the current study results in PEMA with a hydrophilic carboxyl end group. The effects of MWs, polymer concentrations, and terminal groups on the thermal phase transitions of PEMA can then be explored, excluding the interference of broad molecular weight distributions typically encountered with samples prepared by conventional free radical polymerizations. To achieve this, we need to establish firstly that the controlled radical polymerizations of EMA by ATRP and RAFT processes are feasible.

ATRP of EMA

ATRP provides to be a suitable controlled radical polymerization technique as it can provide excellent control over MWs and end groups. The first example of ATRP of *N,N*-disubstituted acrylamide monomers was reported by Teodorescu and Matyjaszewski²¹ for DMA, employing methyl 2-bromopropionate, CuBr, and 1,4,8,11-tetramethyl-1,4,8,11-tetraazacyclotetradecane (Me₄Cyclam) as the initiator, catalyst, and ligand, respectively. They initially concluded that ATRP is not an appropriate technique for the “living” radical polymerization of DMA, which suffers from the deactivation of copper catalyst through complexation with amide groups, displacement of terminal halide atom by amide groups, and low values of ATRP equilibrium constants. Similar conclusions were also obtained by Brittain and coworkers.²⁵

Using improved polymerization conditions, Teodorescu and Matyjaszewski²² later successfully synthesized PDMA with low polydispersity by using methyl 2-chloropropionate as the initiator and CuCl/Me₆TREN as the catalysts. Masci et al.³⁶ then reported the controlled ATRP polymerization of NIPAM in DMF/water mixtures using similar catalysts. Stover and coworkers^{9,10,37,38} further proved that DMA and NIPAM monomers can be controllably polymerized by ATRP at ambient temperature in various alcohols.

Being structurally similar to that of DMA and a structural isomer of NIPAM, EMA is expected to undergo controlled ATRP using alkyl 2-chloropropionate/CuCl/Me₆TREN system. *t*-Butyl alcohol was chosen as the solvent in the current case, because it might protect the catalyst via hydrogen bonding interactions with amide groups of both the EMA monomer and the PEMA polymer [Scheme 1(a)].^{9,10,37,38}

After polymerization at 25 °C for 6 h, the monomer conversion is 79.8%. A typical ¹H NMR spectrum of the purified PEMA recorded in D₂O is shown in Figure 1(b). Resonance signal at 4.1 ppm is ascribed to the methylene protons of terminal ethyl group (CH₃CH₂OCO) resulting from the initiator, ECP. Signals at 3.2–3.6 ppm and 2.7–3.2 ppm are assigned to methylene and methyl protons adjacent to amide groups (NCH₂, NCH₃), respectively. Based on the integral ratios of peak *a* at 4.1 ppm and peak *b*, *c*, and *d* in the range of 2.2–3.6 ppm, the number-average molecular weight ($M_{n,NMR}$) can be calculated according to eq 1:

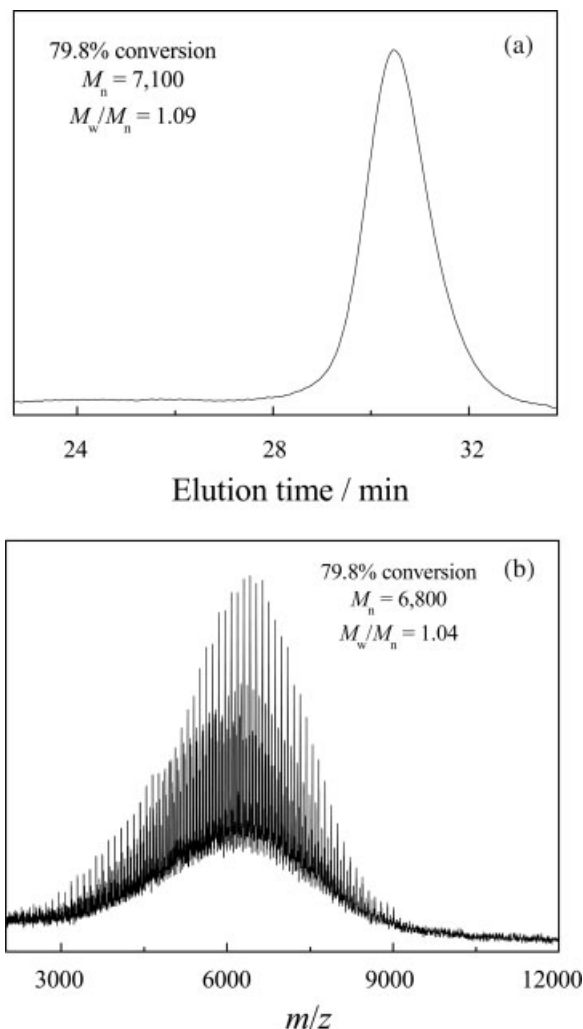


Figure 2. (a) DMF GPC trace and (b) MALDI-TOF MS spectrum obtained for PEMA prepared by the ATRP protocol at a monomer conversion of 79.8%. Polymerization conditions: EMA/*t*-BuOH = 1/2 w/w, [EMA]:[ECP]:[CuCl]:[Me₆TREN] = 80:1:1:1, 25 °C.

$$M_{n,NMR} = \frac{I_{b,c,d}}{3I_a} \times M_{EMA} + M_{init} \quad (1)$$

where $I_{b,c,d}$, I_a , M_{EMA} , and M_{init} are integration areas of resonance peaks *b*, *c*, *d*, and *a*, the molar masses of EMA repeating units and the ATRP initiator, respectively. The number-average molecular weight, M_n , was determined to be 7400 by ¹H NMR.

DMF GPC trace of PEMA homopolymer obtained at a conversion of 79.8% is shown in Figure 2(a), revealing a relatively sharp and symmetric peak. No tailing or shoulder at the lower or higher MW side can be discerned, indicating the absence of premature chain termination. GPC

analysis of PEMA in DMF resulted in an $M_{n, \text{GPC}}$ of 7100 and a polydispersity, M_w/M_n , of 1.09.

The PEMA homopolymer was further analyzed by MALDI-TOF MS and the spectrum was shown in Figure 2(b). Relatively symmetric peak with good resolutions can be observed, extending from 3000 to 9000 Da. The MALDI-TOF MS spectrum gave an M_n value of 6800, which is quite close to that obtained by ^1H NMR and DMF GPC. The M_w/M_n is determined to be 1.04 by MALDI-TOF MS, which is lower than that obtained from GPC (1.09). However, this further confirms that the obtained PEMA possesses a narrow molecular weight distribution.

M_n values determined by GPC, ^1H NMR, and MALDI-TOF MS are quite close to each other, indicating that in the current case, GPC analyses of PEMA samples using DMF as eluent can provide a relatively good estimate of their MWs. To further check whether the ATRP of EMA can be conducted in a controlled manner or not, the polymerization kinetics was investigated. Monomer conversions were determined from the integral ratios of characteristic resonance peaks of vinyl protons (δ 5.6–6.6 ppm, 3H) and that of methyl protons adjacent to the amide group (NCH_3 , δ 2.7–3.2 ppm, 3H). It should be noted that resonance peaks of the polymerization solvent (*t*-butyl alcohol, δ 1.3 ppm) do not overlap with the above two resonance peaks.

The kinetic plot for the ATRP of EMA is shown in Figure 3(a), exhibiting slight curvature with the polymerization time, especially during the early stage of polymerization. However, from Figure 3(b), we can clearly observe the linear increase of M_n with monomer conversions. The polydispersity values slightly decrease with increasing monomer conversions and remain narrow throughout the polymerization (≤ 1.25). Most importantly, the measured M_n values agree quite well with theoretical ones. The linear increase of M_n with monomer conversions suggests that the curvature in the kinetic plots [Fig. 3(a)] is due to progressive catalyst deactivation rather than chain termination.

On the basis of the above kinetic studies, we can conclude that ATRP of EMA monomer can be conducted in a relatively controlled manner, which is similar to that obtained for DMA and NIPAM monomers. However, the overall yield of PEMA after thoroughly removing copper catalyst via passing through neutral alumina column is relatively low ($< 30\%$), although the monomer conversions can be as high as 80% af-

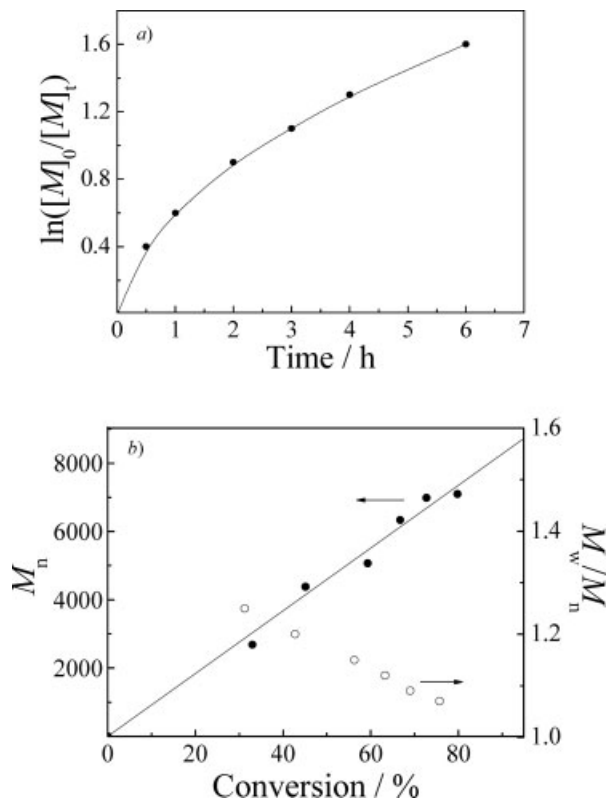


Figure 3. (a) Kinetic plot for the ATRP polymerization of EMA monomer in *t*-BuOH. (b) Variation of the number-average molecular weight, $M_{n, \text{GPC}}$, and polydispersity, M_w/M_n , as a function of monomer conversions. The experimental conditions are the same as those described in Figure 2.

ter 6 h. As the EMA monomer is not commercially available and the starting material, *N*-ethylmethylamine, is quite expensive, we further explored the controlled radical polymerization of EMA via the RAFT process.

RAFT Polymerization of EMA

Since its discovery, RAFT polymerization has been successfully applied to the controlled radical polymerization of various acrylamido monomers such as DMA, NIPAM, and DEA.^{26–29,31–33,39} In 1999, Thang and coworkers^{31,32} reported the first RAFT polymerization of DMA in organic media, in which transfer of a dithioester moiety between active and dormant species endows the “living” character. For both economic and environmental reasons, McCormick and coworkers^{28,29,39} further studied the controlled RAFT polymerization of DMA in aqueous media utilizing dithioesters and trithiocarbonates as chain transfer agents (CTAs). Just recently, Zhu

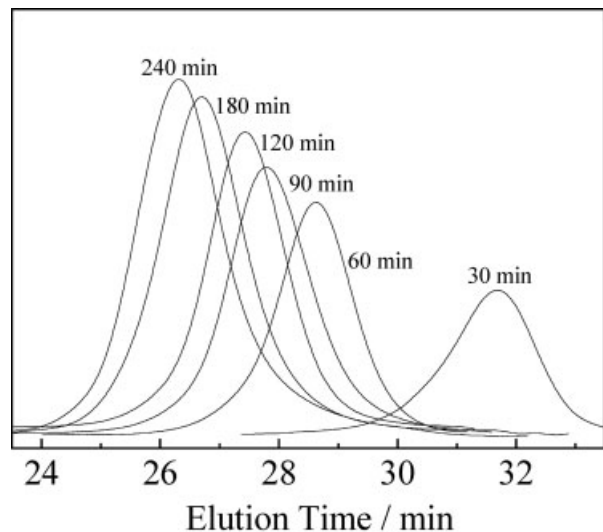


Figure 4. Evolution of GPC traces with polymerization time during the RAFT polymerization of EMA at 80 °C. Polymerization conditions: EMA/1,4-dioxane = 1/2 w/v, [EMA]:[CPAD] = 400:1, [CPAD]:[V-501] = 8:1.

and coworkers³³ reported the RAFT polymerization of DEA using a trithiocarbonate, 2-dodecylsulfanylthiocarbonyl-sulfanyl-2-methylpropionic acid, as the CTA. Good control over the MWs and polydispersities of PDEA was achieved. They also prepared ABC triblock copolymers containing PEMA blocks using poly(*N*-monosubstituted acrylamide) as the macroRAFT agent.

We further studied the RAFT polymerization kinetics of EMA using a dithioester, CPAD, as the CTA. The polymerization was conducted in 1,4-dioxane at 80 °C, targeting for a theoretical DP of 400 [Scheme 1(b)]. At various time intervals, the polymerization was terminated by quenching into liquid nitrogen for subsequent ¹H NMR and GPC analysis. Monomer conversions were estimated based on the integral ratios of resonance peaks of vinyl protons (δ 5.6–6.6 ppm, 3H) to that of methyl protons (CH_2CH_3 , δ 0.9–1.3 ppm, 3H).

The evolution of GPC traces of PEMA obtained at different monomer conversions is shown in Figure 4. We can clearly see that the elution peaks shifted to higher MWs at increasing monomer conversions, which is consistent with a controlled polymerization. Most importantly, all the GPC traces were relatively narrow, mono-modal, and symmetric, revealing the absence of tailing at the lower MW side or a shoulder at the higher MW side. The kinetic plots and the evolution of MWs and polydispersities with monomer conversions were shown in

Figure 5. The monomer conversion reached ~60% after 4 h, the molecular weights increased linearly with conversion, in good agreement with the theoretical values, implying an almost constant concentration of active species during the RAFT polymerization and negligible premature termination of polymeric radicals. We can also observe that the polydispersity of PEMA remains well below 1.2, exhibiting a slight decrease with increasing conversions. This indicates that the RAFT polymerization of EMA can be conducted in a well controlled manner and the molecular weight of the PEMA can be simply controlled by polymerization time.

As both the free radical initiator (V-501) and the RAFT agent (CPAD) contain carboxyl groups, we can assure that all the PEMA chains prepared by the RAFT process bear a terminal carboxyl groups. In the following part, the thermal phase transitions of a series of low-polydispersity PEMA with varying MWs were investigated,

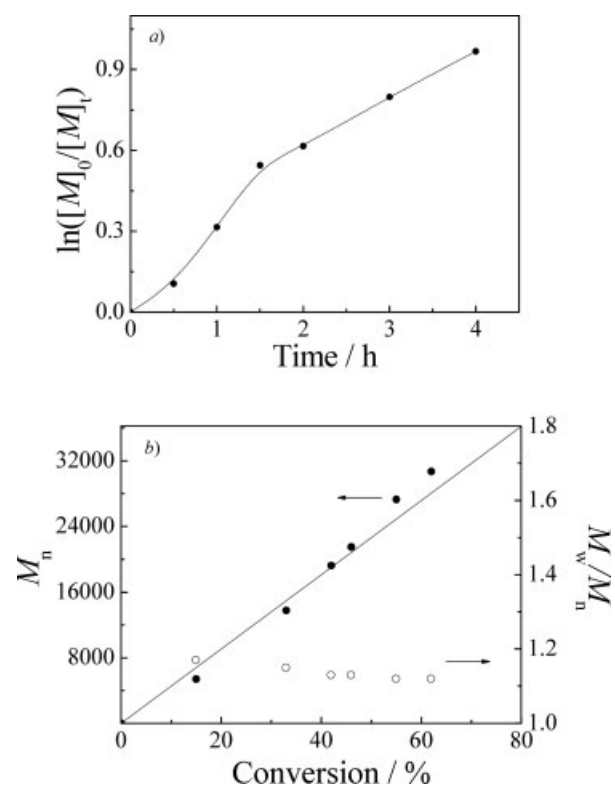


Figure 5. (a) Kinetic plot for the RAFT polymerization of EMA monomer in 1,4-dioxane at 80 °C. (b) Variation of the number-average molecular weight, $M_{n,\text{GPC}}$, and polydispersity, M_w/M_n , as a function of monomer conversion. The experimental conditions are the same as those described in Figure 4.

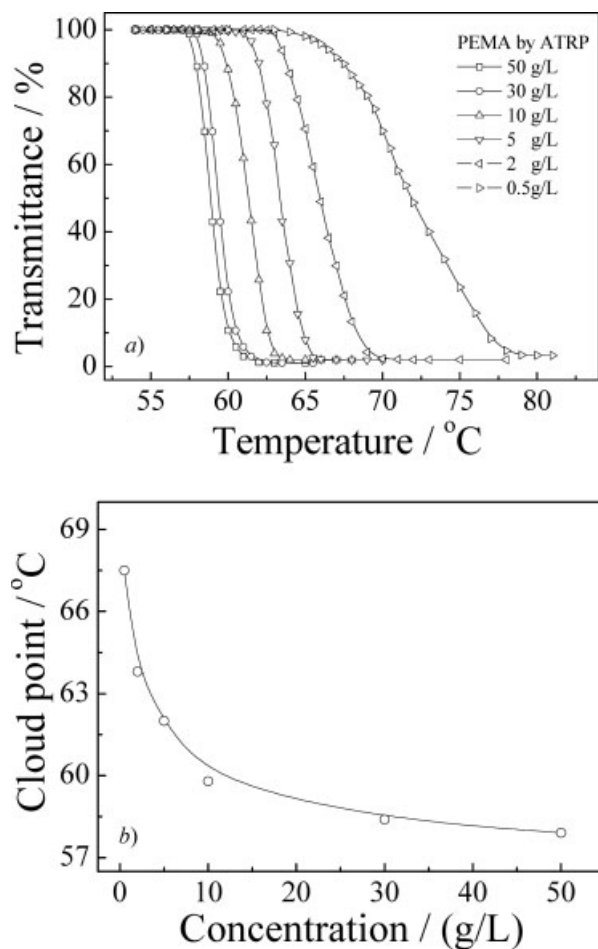


Figure 6. (a) Temperature dependence of optical transmittance at a wavelength of 500 nm obtained for aqueous solutions of PEMA at different concentrations. (b) Variation of cloud points as a function of polymer concentrations. PEMA with an M_n of 7100 and an M_w/M_n of 1.09 was prepared by the ATRP process.

and the effects of MWs, terminal groups, and polymer concentrations were explored.

Thermal Phase Transitions of PEMA Homopolymers

Temperature-dependent turbidimetry was employed to determine the thermal phase transitions of PEMA homopolymers with varying MWs and terminal end groups. CP values were defined as the temperature where a 10% decrease of transmittance can be observed. Generally, CP values of water-soluble polymers may also depend on polymer concentrations, especially for those with low MWs and terminated with hydrophobic groups.^{4,5,10} Figure 6(a) shows temperature-dependent optical transmittance obtained for PEMA homopolymer prepared by

ATRP ($M_{n,GPC} = 7100$, $M_w/M_n = 1.09$) at different concentrations. We can clearly see that CP values increase with decreasing polymer concentrations. As the polymer concentrations decrease from 50 to 0.5 g/L, CP values increase from 58 to 67.5 °C [Fig. 6(b)]. The observed polymer concentration dependences of CPs for PEMA agree quite well with those reported for PNIPAM and poly(2-(2-methoxyethoxy)ethyl methacrylate) (PMEO₂MA).^{5,10}

We can also observe from Figure 6(b) that the increase of CP values is the most prominent at polymer concentrations below 10.0 g/L. To observe the decrease of optical transmittance, chain collapse and subsequent inter-chain aggregation above the LCST should occur, the latter can be greatly facilitated upon increasing polymer concentrations. The CP value is actually a parameter reflecting the point at which macroscopic phase separation takes place.

Chain lengths of water-soluble polymers such as PNIPAM will also affect their thermal phase transitions. However, for PNIPAM, the MW dependence of its CP have been quite controversial. It has been reported that the CP values can increase,^{40,41} decrease,^{9,10,42,43} or remain unaffected^{44–46} with increasing MWs, partially because of that PNIPAM samples were prepared by different polymerization methods and some of them were actually quite polydisperse in molecular weight distributions. However, Stover and coworkers^{9,10} recently clarified this issue by using a series of well-defined PNIPAM samples with varying MWs prepared by ATRP.

The thermal phase transitions of a series of low-polydispersity PEMA samples with different MWs at a fixed concentration (10 g/L) were studied. We can observe from Figure 7 that MWs exhibit considerable effects on the CPs of PEMA. As M_n increases from 5400 to 36,500, the CP drops from 64.5 to 59.5 °C [Fig. 7(b)]. This was in general agreement with those obtained for PNIPAM and PME₂O₂MA as reported by Stover and coworkers^{9,10} and Lutz et al.⁵

We can also deduce from Figure 7(b) that PEMA homopolymer with an M_n of 7100 (prepared by RAFT process) would possess a CP value of ~64 °C at a concentration of 10 g/L. Interestingly, PEMA with comparable MW exhibits a CP of ~60 °C at the same polymer concentrations (Fig. 6). PEMA sample prepared by ATRP possesses —Cl end group stemming from the initiator (ECP), while polymers pre-

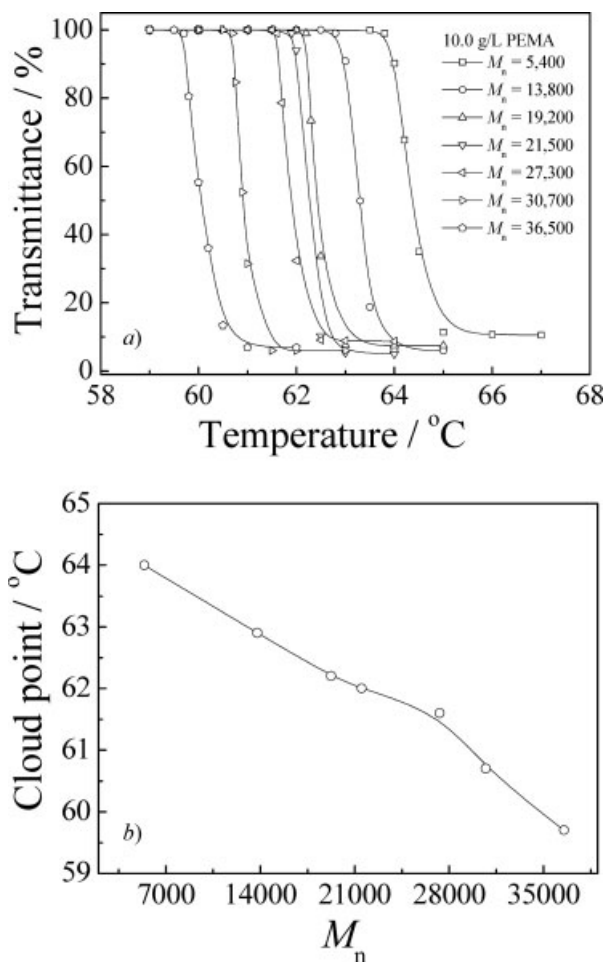


Figure 7. (a) Temperature dependence of optical transmittance at 500 nm obtained for aqueous solutions of PEMA with different molecular weights. (b) Variation of cloud points as a function of the molecular weights. PEMA homopolymers were prepared by RAFT polymerization and the polymer concentration was fixed at 10.0 g/L.

pared by RAFT polymerization bear a carboxyl terminal group. Thus, the much higher CP value for PEMA prepared by the RAFT technique compared with that by ATRP should be ascribed to the presence of hydrophilic carboxyl group at the chain end for the former. It has been well-established that the LCST of PNIPAM can increase or decrease upon random or block copolymerization with hydrophilic or hydrophobic monomers. Similarly, the presence of hydrophilic terminal groups should also elevate the phase transition temperatures.

The tacticity of the water-soluble polymer might also affect their LCST phase behavior.⁴ To make sure that the end group effect described above was not due to differences in tacticity, we

further checked the stereochemistry of the two types of PEMA samples prepared by ATRP and RAFT processes. ¹H NMR spectra (500 MHz, D₂O) revealed resonance signals characteristic of methylene protons of isotactic PEMA (*meso*, *m*) at 1.15 and 1.64 ppm, and signals at 1.29 and 1.57 ppm characteristic of methylene protons of syndiotactic PEMA (*racemic*, *r*) (data not shown). The *m/r* values of PEMA samples prepared by ATRP ($M_{n, GPC} = 7100$) and by RAFT ($M_{n, GPC} = 5400$) were $\sim 46/54$ and $\sim 48/52$, respectively. This indicated that PEMA samples prepared by ATRP and RAFT processes possessed the same stereochemistry.

To the best of our knowledge, this represents the first systematic investigation of the thermal phase transitions of PEMA samples. It seems that for thermoresponsive water-soluble acrylamido-based polymers, the effects of MWs, polymer concentrations, and end groups on the CPs can be generalized, that is, CP increases with decreasing polymer concentrations, MWs, and hydrophobicity of terminal groups.

CONCLUSIONS

In summary, the controlled radical polymerizations of EMA by ATRP and RAFT processes were systematically investigated for the first time. In both cases, the polymerization can be conducted in a “controlled” manner, as revealed by the narrow polydispersity of PEMA and the linear increase of MWs with monomer conversions. Moreover, the thermal phase transitions of a series of low-polydispersity PEMA samples with varying MWs and terminal groups were also studied. The effects of MWs, polymer concentrations, and hydrophobicity/hydrophilicity of end groups on the CP values of PEMA homopolymer were systematically explored. CPs of PEMA generally increase with decreasing polymer concentrations, MWs, and hydrophobicity of terminal groups.

This work was financially supported by an Outstanding Youth Fund (50425310) and research grants (20534020 and 20674079) from the National Natural Scientific Foundation of China (NNSFC), the “Bai Ren” Project of the Chinese Academy of Sciences, and the Program for Changjiang Scholars and Innovative Research Team in University (PCSIRT).

REFERENCES AND NOTES

- Gil, E.; Hudson, S. *Prog Polym Sci* 2004, 29, 1173–1222.

2. Galaev, I.; Mattiasson, B. *Enzyme Microb Tech* 1993, 15, 354–366.
3. Freitag, R.; Baltes, T.; Eggert, M. *J Polym Sci Part A: Polym Chem* 1994, 32, 3019–3030.
4. Furyk, S.; Zhang, Y.; Ortiz-Acosta, D.; Cremer, P.; Bergbreiter, D. *J Polym Sci Part A: Polym Chem* 2006, 44, 1492–1501.
5. Lutz, J.; Akdemir, O.; Hoth, A. *J Am Chem Soc* 2006, 128, 13046–13047.
6. Duan, Q.; Miura, Y.; Narumi, A.; Shen, X.; Sato, S.; Satoh, T.; Kakuchi, T. *J Polym Sci Part A: Polym Chem* 2006, 44, 1117–1124.
7. Iijima, M.; Nagasaki, Y. *J Polym Sci Part A: Polym Chem* 2006, 44, 1457–1469.
8. Zhang, Y.; Furyk, S.; Sagle, L. B.; Cho, Y.; Bergbreiter, D. E.; Cremer, P. S. *J Phys Chem C* 2007, 111, 8916–8924.
9. Xia, Y.; Yin, X.; Burke, N.; Stover, H. *Macromolecules* 2005, 38, 5937–5943.
10. Xia, Y.; Burke, N.; Stover, H. *Macromolecules* 2006, 39, 2275–2283.
11. Barner-Kowollik, C.; Buback, M.; Charleux, B.; Coote, M. L.; Drache, M.; Fukuda, T.; Goto, A.; Klumperman, B.; Lowe, A. B.; Mcleary, J. B.; Moad, G.; Monteiro, M. J.; Sanderson, R. D.; Tonge, M. P.; Vana, P. *J Polym Sci Part A: Polym Chem* 2006, 44, 5809–5831.
12. Hawker, C. J.; Wooley, K. L. *Science* 2005, 309, 1200–1205.
13. O'Reilly, R. K.; Joralemon, M. J.; Hawker, C. J.; Wooley, K. L. *J Polym Sci Part A: Polym Chem* 2006, 44, 5203–5217.
14. Perrier, S.; Takolpuckdee, P. *J Polym Sci Part A: Polym Chem* 2005, 43, 5347–5393.
15. Idziak, I.; Avoce, D.; Lessard, D.; Gravel, D.; Zhu, X. X. *Macromolecules* 1999, 32, 1260–1263.
16. Maeda, Y.; Nakamura, T.; Ikeda, I. *Macromolecules* 2002, 35, 217–222.
17. Eggert, M.; Freitag, R. *J Polym Sci Part A: Polym Chem* 1994, 32, 803–813.
18. Ito, S.; Mizogushi, K.; Suda, Y. *Bull Res Inst Polym Text* 1984, 144, 7–23.
19. Panayiotou, M.; Garret-Flaudy, F.; Freitag, R. *Polymer* 2004, 45, 3055–3061.
20. Kobayashi, M.; Okuyama, S.; Ishizone, T.; Nakahama, S. *Macromolecules* 1999, 32, 6466–6477.
21. Teodorescu, M.; Matyjaszewski, K. *Macromolecules* 1999, 32, 4826–4831.
22. Teodorescu, M.; Matyjaszewski, K. *Macromol Rapid Commun* 2000, 21, 190–194.
23. Lutz, J.; Neugebauer, D.; Matyjaszewski, K. *J Am Chem Soc* 2003, 125, 6986–6993.
24. Neugebauer, D.; Matyjaszewski, K. *Macromolecules* 2003, 36, 2598–2603.
25. Rademacher, J.; Baum, R.; Pallack, M.; Brittain, W.; Simonsick, W. *Macromolecules* 2000, 33, 284–288.
26. Baum, M.; Brittain, W. *Macromolecules* 2002, 35, 610–615.
27. Donovan, M.; Lowe, A.; Sumerlin, B.; McCormick, C. *Macromolecules* 2002, 35, 4123–4132.
28. Donovan, M.; Sanford, T.; Lowe, A.; Sumerlin, B.; Mitsukami, Y.; McCormick, C. *Macromolecules* 2002, 35, 4570–4572.
29. Convertine, A.; Lokitz, B.; Lowe, A.; Scales, C.; Myrick, L.; McCormick, C. *Macromol Rapid Commun* 2005, 26, 791–795.
30. Lowe, A. B.; McCormick, C. L. *Prog Polym Sci* 2007, 32, 283–351.
31. Chong, Y.; Le, T.; Moad, G.; Rizzardo, E.; Thang, S. *Macromolecules* 1999, 32, 2071–2074.
32. Rizzardo, E.; Chiefari, J.; Mayadunne, R.; Moad, G.; Thang, S. *Macromol Symp* 2001, 174, 209–212.
33. Cao, Y.; Zhu, X. X. *Can J Chem* 2007, 85, 407–411.
34. Ciampolini, M.; Nardi, N. *Inorg Chem* 1966, 5, 41–44.
35. Mitsukami, Y.; Donovan, M.; Lowe, A.; McCormick, C. *Macromolecules* 2001, 34, 2248–2256.
36. Masci, G.; Giacomelli, L.; Crescenzi, V. *Macromol Rapid Commun* 2004, 25, 559–564.
37. Yin, X.; Stover, H. *Macromolecules* 2003, 36, 9817–9822.
38. Yin, X.; Stover, H. *Macromolecules* 2005, 38, 2109–2115.
39. Convertine, A.; Lokitz, B.; Vasileva, Y.; Myrick, L.; Scales, C.; Lowe, A.; McCormick, C. *Macromolecules* 2006, 39, 1724–1730.
40. Zheng, X.; Tong, Z.; Xie, X.; Zeng, F. *Polym J* 1998, 30, 284–288.
41. Tong, Z.; Zeng, F.; Zheng, X.; Sato, T. *Macromolecules* 1999, 32, 4488–4490.
42. Schild, H.; Tirrell, D. *J Phys Chem* 1990, 94, 4352–4356.
43. Baltes, T.; Garret-Flaudy, F.; Freitag, R. *J Polym Sci Part A: Polym Chem* 1999, 37, 2977–2989.
44. Fujishige, S.; Kubota, K.; Ando, I. *J Phys Chem* 1989, 93, 3311–3313.
45. Tiktopulo, E.; Uversky, V.; Lushchik, V.; Klenin, S.; Bychkova, V.; Ptitsyn, O. *Macromolecules* 1995, 28, 7519–7524.
46. Ding, Z.; Chen, G.; Hoffman, A. *Bioconjugate Chem* 1996, 7, 121–125.